The Treatment of Time Continuous GPS Observations for the Determination of Regional Deformation Parameters

Ludovico Biagi[(1)] and Athanasios Dermanis[(2)]

[(1)] DIIAR, c/o Polo regionale di Como, Politecnico di Milano,
[(2)] Department of Geodesy and Surveying, The Aristotle University of Thessaloniki

Abstract

The calculation of invariant deformation parameters, entering in the constitutional equations of crustal dynamics, requires information on the geometry of the crust in the study region, which is continuous in both the time and spatial domain. The use of continuously observing GPS stations provides geodetic data which are practically time-continuous and must be only spatially interpolated. A strategy is developed for the treatment of dense series of horizontal coordinates from a regional GPS network, which are typically exhibiting a time-linear behavior. The role of the choice of reference system is examined for the removal of trend before the spatial interpolation as well as the determination of the motion of the region as whole with respect to the ITRF or of the relative motion of tectonically homogeneous sub regions. Rigorous formulas are presented for various horizontal deformation parameters and their intrinsic time derivatives, without the usual infinitesimal approximations. Finally the problem of quality assessment for the derived parameters is investigated completely ignoring the questionable formal statistical characteristic of the original geodetic data. A realistic numerical example demonstrates the suggested techniques, involving spatial interpolation by the classical finite-element method. A software package in standard C language has been developed in order to implement the proposed algorithms.

1 Introduction

Although crustal deformation is naturally a three-dimensional (3D) phenomenon, there is a long tradition of a two-dimensional (2D) treatment of the relevant data, primarily by the finite element method using horizontal triangles within which deformation is assumed to be homogeneous. This restriction is partly due to the difficulty of obtaining high quality leveling data, or nowadays in the lower quality of heights from GPS observations. The main reason though is that our discrete positional information is fundamentally 2D as restricted to the surface of the earth. Interpolation can provide continuous information in the surface or horizontal sense, but extension to the 3D unknown deformation requires an extrapolation in the surface-normal or height sense, which is not justified for the available data.

The derivation of horizontal deformation, ignoring height information is somewhat unnatural since it is not concerned with the deformation of the material points constituting the crust, but rather with the deformation of their projections on a horizontal reference surface. The results are more realistic when the surface is essentially flat and height variations do not alter height differences in the area, i.e. the whole area is uplifted or down-lifted as a whole. Only in this case horizontal deformation is the horizontal trace of the actual 3D deformation.

A realistic treatment must study the deformation of the 2D natural earth surface as embedded in 3D space and provide the "trace" of the unknown 3D deformation in the tangent plane for each surface point. This generalized treatment will be presented elsewhere. For the time being we mention an obvious extension of the finite element method in the "right direction". In Dermanis (1994) we have presented a version of the finite element method where, instead of coordinates the horizontal distances of the triangle sides at epochs are used. If the horizontal distances are replaced by spatial distances taking also height information into account, more realistic deformation parameters can be computed, which are referring to the tangential rather than the horizontal trace of the actual 3D deformation.

In any case, here we will follow the traditional restriction of the horizontal treatment, since our aim is to update some existing computational techniques (Dermanis & Livieratos, 1983, Dermanis & Rossikopoulos,1988, Rossikopoulos, 2001), in a direction which takes into account the nature of presently available data from permanent GPS stations monitoring a deforming area. The daily network solutions, apart from some missing or obvious outlier days, manifest a linear evolution in time, even for

long periods up to 2 years. This is not surprising, since the motions of "floating" tectonic plates are rotations around a fixed axis. Furthermore they are so slow that the displacements, circular in principle, appear to be linear in the "infinitesimal" time interval of few years, especially for points far away from the plate-rotation axis, which may well be located outside the plate itself. The use of a "constant velocity" model for the station coordinates as functions of time provides a surplus of data that allows us to address the data quality assessment problem, completely ignoring the unrealistic (specially when derived from GPS observations) formal covariance matrices accompanying the daily network solutions.

2 Horizontal Deformation Parameters

Deformation is primarily described by the deformation function $\mathbf{f}$, which relates the coordinates $\mathbf{x} = \mathbf{f}(\mathbf{x}_0)$ of any material point at some particular epoch t to the coordinates $\mathbf{x}_0$ of the same material point at some reference epoch t_0. In the differential equations of motion, which connect the deformation of a material body under external forces with its response characteristics (constitutional equations), the deformation function enters through its local linear approximation, the deformation gradient $\mathbf{F} = \frac{\partial \mathbf{f}}{\partial \mathbf{x}_0} = \frac{\partial \mathbf{x}}{\partial \mathbf{x}_0}$. The linear mapping $\mathbf{F}$ describes how each curve changes its spatial direction and rate of length variation, by mapping a tangent vector to a curve at epoch t_0 to the tangent vector to its new position at epoch t .The deformation gradient depends on the chosen reference systems. Under system changes described by $\tilde{\mathbf{x}} = \mathbf{S}\mathbf{x}$, $\tilde{\mathbf{x}}_0 = \mathbf{S}_0\mathbf{x}_0$, the deformation gradient is represented by the new matrix $\tilde{\mathbf{F}} = \mathbf{S}\mathbf{F}\mathbf{S}_0^T$. In order to get an insight into the nature of the deformation gradient independently of the coordinate systems involved, we will resort to the singular value decomposition (SVD)

$$\mathbf{F} = \mathbf{Q}^T \mathbf{\Lambda} \mathbf{P} \tag{1}$$

where $\mathbf{P}$, $\mathbf{Q}$ are orthogonal matrices and $\mathbf{\Lambda}$ a diagonal matrix having diagonal elements the singular values $\lambda_i = \Lambda_{ii}$ of $\mathbf{F}$. These are related to the diagonalization of two symmetric matrices, the right Cauchy strain matrix

$$\mathbf{C} = \mathbf{F}^T\mathbf{F} = \mathbf{P}^T\mathbf{\Lambda}^2\mathbf{P} \tag{2}$$

and the left Cauchy strain matrix

$$\mathbf{B} = \mathbf{F}\mathbf{F}^T = \mathbf{Q}^T\mathbf{\Lambda}^2\mathbf{Q}. \tag{3}$$

Thus the columns of $\mathbf{P}^T$ are the eigenvectors of $\mathbf{C}$, the columns of $\mathbf{Q}^T$ are the eigenvectors of $\mathbf{B}$ and the diagonal elements $\lambda_i^2 = (\mathbf{\Lambda}^2)_{ii} = \Lambda_{ii}^2$ are the common eigenvalues of $\mathbf{C}$ and $\mathbf{B}$, arranged in order of magnitude from larger to smaller. Related to the SVD is the polar decomposition

$$\mathbf{F} = \mathbf{R}\mathbf{U} = \mathbf{V}\mathbf{R}, \tag{4}$$

which involves the right stretch matrix

$$\mathbf{U} = \mathbf{P}^T\mathbf{\Lambda}\mathbf{P} = \mathbf{C}^{1/2} \tag{5}$$

the left stretch matrix

$$\mathbf{V} = \mathbf{Q}^T\mathbf{\Lambda}\mathbf{Q} = \mathbf{B}^{1/2} \tag{6}$$

and the rotation matrix

$$\mathbf{R} = \mathbf{Q}^T\mathbf{P}. \tag{7}$$

Most common in engineering applications is the use of the strain matrix

$$\mathbf{E} = \tfrac{1}{2}(\mathbf{C} - \mathbf{I}) = \mathbf{P}^T[\tfrac{1}{2}(\mathbf{\Lambda}^2 - \mathbf{I})]\mathbf{P} \tag{8}$$

with eigenvalues $\frac{1}{2}(\lambda_i^2 - 1)$, or its infinitesimal approximation

$$\mathbf{E}_{\text{inf}} = \tfrac{1}{2}(\mathbf{J} + \mathbf{J}^T) = \mathbf{E} - \tfrac{1}{2}\mathbf{J}\mathbf{J}^T \tag{9}$$

expressed in terms of the displacement gradient

$$\mathbf{J} = \frac{\partial \mathbf{u}}{\partial \mathbf{x}_0} = \frac{\partial(\mathbf{x} - \mathbf{x}_0)}{\partial \mathbf{x}_0} = \frac{\partial \mathbf{x}}{\partial \mathbf{x}_0} - \frac{\partial \mathbf{x}_0}{\partial \mathbf{x}_0} = \mathbf{F} - \mathbf{I}, \tag{10}$$

in equation (9) the quadratic terms $\frac{1}{2}\mathbf{J}\mathbf{J}^T$ are neglected.

It can be easily shown that under a change of reference frames the above matrices are replaced by $\tilde{\mathbf{F}} = \mathbf{S}\mathbf{F}\mathbf{S}_0^T$, $\tilde{\mathbf{C}} = \mathbf{S}_0\mathbf{C}\mathbf{S}_0^T$, $\tilde{\mathbf{B}} = \mathbf{S}\mathbf{B}\mathbf{S}^T$, $\tilde{\mathbf{R}} = \mathbf{S}\mathbf{R}\mathbf{S}_0^T$, $\tilde{\mathbf{Q}} = \mathbf{Q}\mathbf{S}^T$, $\tilde{\mathbf{P}} = \mathbf{P}\mathbf{S}_0^T$ and $\tilde{\mathbf{\Lambda}} = \mathbf{\Lambda}$. The only invariants are the singular values $\tilde{\lambda}_i = \lambda_i$. The matrix $\mathbf{P}$ transforms the direction of the axes of the coordinate system at epoch t_0 to the directions of the eigenvectors of $\mathbf{C}$, which are physical invariants called *principal directions*. Points at these directions are displaced along the same directions so that their distances from the reference point change by factors λ_i. After this deformation the area around

the reference point is rotated as described by the matrix $\mathbf{R}$.

In the horizontal treatment the SVD becomes

$$\mathbf{F} = \mathbf{R}(-\theta_Q)\mathbf{\Lambda}\mathbf{R}(\theta_P) \tag{11}$$

explicitly

$$\begin{bmatrix} F_{11} & F_{12} \\ F_{21} & F_{22} \end{bmatrix} = \tag{12}$$

$$= \begin{bmatrix} \cos\theta_Q & -\sin\theta_Q \\ \sin\theta_Q & \cos\theta_Q \end{bmatrix} \begin{bmatrix} \lambda_1 & 0 \\ 0 & \lambda_2 \end{bmatrix} \begin{bmatrix} \cos\theta_P & \sin\theta_P \\ -\sin\theta_P & \cos\theta_P \end{bmatrix}$$

The singular values and the angle θ_P, computed by the well known solution of the 2D diagonalization problem $\mathbf{C} = \mathbf{R}(-\theta_P)\mathbf{\Lambda}^2\mathbf{R}(\theta_P)$ are

$$\lambda_1^2 = \frac{C_{11}+C_{22}}{2} + \sqrt{\left(\frac{C_{11}-C_{22}}{2}\right)^2 + C_{12}^2} \tag{13}$$

$$\lambda_2^2 = \frac{C_{11}+C_{22}}{2} - \sqrt{\left(\frac{C_{11}-C_{22}}{2}\right)^2 + C_{12}^2} \tag{14}$$

$$\tan 2\theta_P = \frac{C_{12}}{\frac{1}{2}(C_{11}-C_{22})}, \tag{15}$$

where $C_{11} = F_{11}^2 + F_{21}^2$, $C_{22} = F_{12}^2 + F_{22}^2$, $C_{12} = F_{11}F_{12} + F_{21}F_{22}$. If the strain matrix is used then

$$\lambda_1^2 = 1 + (E_{11}+E_{22}) + \sqrt{(E_{11}-E_{22})^2 + 4E_{12}^2} \tag{16}$$

$$\lambda_2^2 = 1 + (E_{11}+E_{22}) - \sqrt{(E_{11}-E_{22})^2 + 4E_{12}^2} \tag{17}$$

$$\tan 2\theta_P = \frac{2E_{12}}{E_{11}-E_{22}}. \tag{18}$$

Instead of the singular values which are scale factors along the principal direction, more appealing to the engineering visualization of deformation seem to be the dilatation Δ (percentage of area change) and shear γ, which relates to the distortion of a square into an oblique parallelogram with bases along the same straight lines, skewed by an angle having γ as its tangent.

A shear along the *x*-axis is represented by the shear matrix

$$\mathbf{\Gamma} = \begin{bmatrix} 1 & \gamma \\ 0 & 1 \end{bmatrix} \tag{19}$$

and a shear in the direction with angle ϕ by the matrix

$$\mathbf{\Gamma}_\phi = \mathbf{R}(-\phi)\mathbf{\Gamma}\mathbf{R}(\phi). \tag{20}$$

The 4-parameters deformation gradient $\mathbf{F}$ can be represented by a shear γ in direction ϕ, a scale factor s and an additional rotation by an angle ψ

$$\mathbf{F} = s\mathbf{R}(\psi)\mathbf{\Gamma}_\phi = s\mathbf{R}(\psi)\mathbf{R}(-\phi)\mathbf{\Gamma}\mathbf{R}(\phi). \tag{21}$$

Since $|\mathbf{\Gamma}| = 1$ and all orthogonal rotation matrices have determinant 1 too, the scale factor is directly determined from the determinant

$$s = \sqrt{|\mathbf{F}|} = \sqrt{F_{11}F_{22} - F_{12}F_{21}}, \tag{22}$$

and is related to the singular values by $s^2 = |\mathbf{F}| = |\mathbf{P}^T||\mathbf{\Lambda}||\mathbf{Q}| = |\mathbf{\Lambda}| = \lambda_1\lambda_2$ and

$$s = \sqrt{\lambda_1\lambda_2}. \tag{23}$$

The shear can then be determined from

$$tr\mathbf{C} = tr(\mathbf{F}^T\mathbf{F}) = s^2 tr\{\mathbf{R}(-\phi)\mathbf{\Gamma}^T\mathbf{\Gamma}\mathbf{R}(\phi)\} =$$

$$= s^2 \mathrm{tr}\{\mathbf{\Gamma}^T\mathbf{\Gamma}\mathbf{R}(\phi)\mathbf{R}(-\phi)\} = s^2 \mathrm{tr}\{\mathbf{\Gamma}^T\mathbf{\Gamma}\} =$$

$$= s^2 \mathrm{tr}\begin{bmatrix} 1 & \gamma \\ \gamma & 1+\gamma^2 \end{bmatrix} = s^2(2+\gamma^2) = \mathrm{tr}(\mathbf{Q}^T\mathbf{\Lambda}^2\mathbf{Q}) =$$

$$= \mathrm{tr}(\mathbf{\Lambda}^2\mathbf{Q}\mathbf{Q}^T) = \mathrm{tr}(\mathbf{\Lambda}^2) = \lambda_1^2 + \lambda_2^2 \tag{24}$$

and

$$\gamma = \sqrt{\frac{C_{11}+C_{22}}{s^2} - 2} = \sqrt{\frac{\lambda_1^2+\lambda_2^2}{\lambda_1\lambda_2} - 2} = \frac{\lambda_1-\lambda_2}{\sqrt{\lambda_1\lambda_2}} \tag{25}$$

To determine the direction of shear ϕ we use the SVD of $\mathbf{\Gamma}$:

$$\mathbf{\Gamma} = \mathbf{R}'^T_\Gamma \mathbf{M}\mathbf{R}_\Gamma = \mathbf{R}(-\theta'_\Gamma)\begin{bmatrix} \mu_1 & 0 \\ 0 & \mu_2 \end{bmatrix}\mathbf{R}(\theta_\Gamma) \tag{26}$$

The diagonalization problem

$$\mathbf{\Gamma}^T\mathbf{\Gamma} = \mathbf{R}_\Gamma{}^T\mathbf{M}^2\mathbf{R}_\Gamma \tag{27}$$

gives

$$\tan 2\theta_\Gamma = \frac{2}{-\gamma}. \tag{28}$$

Comparison with the SVD of $\mathbf{F}$

$$\mathbf{F} = s\mathbf{R}(\psi-\phi-\theta'_\Gamma)\mathbf{M}\mathbf{R}(\theta_\Gamma+\phi) = \\ = \mathbf{R}(-\theta_Q)\mathbf{\Lambda}\mathbf{R}(\theta_P) \tag{29}$$

establishes the relation

$$\phi = \theta_P - \theta_\Gamma. \tag{30}$$

3 Propagation of Variances and Covariances

Starting from the complete covariance matrix of the elements of the deformation gradient $\mathbf{F}$ it is possible to compute covariance matrices for other deformation parameters in steps, as follows

$$\mathbf{F} \rightarrow \mathbf{C} \rightarrow \{\lambda_1,\lambda_2,\theta_P\} \rightarrow \{\gamma,\Delta,\phi\}$$

utilizing at each step the following relevant partial derivatives:

$$\frac{\partial\begin{bmatrix}C_{11}\\C_{12}\\C_{22}\end{bmatrix}}{\partial\begin{bmatrix}F_{11}\\F_{12}\\F_{21}\\F_{22}\end{bmatrix}} = \begin{bmatrix}2F_{11} & 0 & 2F_{21} & 0\\ F_{12} & F_{11} & F_{22} & F_{21}\\ 0 & 2F_{12} & 0 & 2F_{22}\end{bmatrix} \tag{31}$$

$$\frac{\partial\begin{bmatrix}\lambda_1\\\lambda_2\\\theta_P\end{bmatrix}}{\partial\begin{bmatrix}C_{11}\\C_{12}\\C_{22}\end{bmatrix}} = \begin{bmatrix}\frac{1}{4\lambda_1}\left(1+\frac{K}{B}\right) & \frac{C_{12}}{2\lambda_1 B} & \frac{1}{4\lambda_1}\left(1-\frac{K}{B}\right)\\ \frac{1}{4\lambda_2}\left(1-\frac{K}{B}\right) & -\frac{C_{12}}{2\lambda_2 B} & \frac{1}{4\lambda_2}\left(1+\frac{K}{B}\right)\\ -\frac{C_{12}}{4B^2} & \frac{K}{2B^2} & \frac{C_{12}}{4B^2}\end{bmatrix} \tag{32}$$

where $K = (C_{11}-C_{22})/2$ and $B = \sqrt{K^2+C_{12}^2}$,

$$\frac{\partial\begin{bmatrix}\gamma\\\Delta\\\phi\end{bmatrix}}{\partial\begin{bmatrix}\lambda_1\\\lambda_2\\\theta_P\end{bmatrix}} = \begin{bmatrix}\frac{\lambda_1+\lambda_2}{2\lambda_1\sqrt{\lambda_1\lambda_2}} & -\frac{\lambda_1+\lambda_2}{2\lambda_2\sqrt{\lambda_1\lambda_2}} & 0\\ \lambda_2 & \lambda_1 & 0\\ -\frac{\gamma\lambda_2}{4B} & \frac{\gamma\lambda_1}{4B} & 1\end{bmatrix} \tag{33}$$

4 Interpolation of Displacements Using the Finite Element Method

The simplest way to interpolate displacements determined at the vertices of a control network, is by assuming that it is homogenous within properly formulated network triangles, serving as finite elements. The interpolation model has the form

$$\begin{bmatrix}U\\V\end{bmatrix} = \begin{bmatrix}J_{11} & J_{12}\\ J_{21} & J_{22}\end{bmatrix}\begin{bmatrix}X\\Y\end{bmatrix} + \begin{bmatrix}g_x\\g_y\end{bmatrix}. \tag{34}$$

The elements J_{ik} of the displacement gradient matrix, which are constant within each triangle, are recovered from the known displacement values (U_i,V_i) at the triangle vertices having coordinates (X_i,Y_i), $i = A,B,C$, using the relations

$$J_{11} = \frac{(Y_B-Y_C)U_A+(Y_C-Y_A)U_B-(Y_B-Y_A)U_C}{D}$$

$$J_{12} = \frac{(X_C-X_B)U_A-(X_C-X_A)U_B+(X_B-X_A)U_C}{D}$$

$$J_{21} = \frac{(Y_B-Y_C)V_A+(Y_C-Y_A)V_B-(Y_B-Y_A)V_C}{D}$$

$$J_{22} = \frac{(X_C-X_B)V_A-(X_C-X_A)V_B+(X_B-X_A)V_C}{D} \tag{35}$$

where

$$D = (X_B-X_A)(Y_C-Y_A)-(X_C-X_A)(Y_B-Y_A). \tag{36}$$

From the displacement gradient $\mathbf{J}$, the deformation gradient $\mathbf{F} = \mathbf{I}+\mathbf{J}$ can be computed, from which all relevant deformation parameters can be derived. The complete covariance matrix of the network velocities and coordinates can be used in order to compute the complete covariance matrix of the elements of $\mathbf{F}$, by covariance propagation for

all triangles, and proceed on for the covariances of other deformation parameters. To perform the covariance propagation from the coordinates and displacements to the elements F_{ij}, we need the relevant partial derivatives. In fact we need only those with respect to the displacements, since the ones referring to coordinates are too small to be of any practical importance. The required derivatives for this first step of covariance propagation $(U_i, V_i \rightarrow \mathbf{F})$ are

$$\frac{\partial[F_{11}\, F_{12}\, F_{21}\, F_{22}]^T}{\partial[U_A\, V_A\, U_B\, V_B\, U_C\, V_C]^T} =$$

$$= \begin{bmatrix} \frac{Y_B - Y_C}{D} & 0 & \frac{Y_C - Y_A}{D} & 0 & \frac{Y_A - Y_B}{D} & 0 \\ \frac{X_C - X_B}{D} & 0 & \frac{X_A - X_C}{D} & 0 & \frac{X_B - X_A}{D} & 0 \\ 0 & \frac{Y_B - Y_C}{D} & 0 & \frac{Y_C - Y_A}{D} & 0 & \frac{Y_A - Y_B}{D} \\ 0 & \frac{X_C - X_B}{D} & 0 & \frac{X_A - X_C}{D} & 0 & \frac{X_B - X_A}{D} \end{bmatrix} \tag{37}$$

5 The Case of Linearly Moving Permanent GPS Stations

In a permanent GPS network, daily or weekly solutions provide coordinates which exhibit a linear trend with superimposed noise. Each separate single-epoch solution is accompanied by a complete covariance matrix for all coordinates of all network points, which presumably reflect the attained accuracy, while coordinate estimates for different epochs are formally uncorrelated since they are computed from different observations which are presumably uncorrelated. On the other hand such estimate statistics are commonly recognized to be overoptimistic and therefore unrealistic, since unknown biases affecting the observations are not taken into account. For this reason we propose to discard the available covariance matrices and to perform an independent variance-covariance component estimation utilizing the residuals resulting after fitting a linear model to each point coordinate.

Some simplifying assumptions are necessary to arrive to a computationally reasonable and efficient algorithm, which of course may be subject to criticism. In any case we claim that at least they offer an attractive alternative to the use of the formal unrealistic variances and covariance coming from the network per epoch adjustments. Explicitly we assume that network performance does not vary essentially with time while different epoch estimates remain uncorrelated. The first assumption is supported from the analysis of coordinate series from daily solutions. For the second one we note that a small correlation is present between consecutive days. A refined procedure seeking also an estimate of this correlation will be the object of future work.

We outline the suggested procedure taking into account only horizontal coordinates X, Y, the extension to three coordinates being straightforward. The linear trend model is

$$X_{ki} \equiv X(P_k, t_i) = X_{0k} + U_k (t_i - t_0) + v_{X_k t_i}$$

$$Y_{ki} \equiv Y(P_k, t_i) = Y_{0k} + V_k (t_i - t_0) + v_{Y_k t_i} \tag{38}$$

for network points P_k, $i = 1, 2, \ldots, M$, at epochs t_i, $i = 1, 2, \ldots, N$, where X_{0k}, Y_{0k} are the initial coordinates of point P_k at the chosen reference epoch t_0 and U_k, V_k the corresponding constant velocity components. We explicitly assume that

$$E\{v_{Xki}\} = 0\,,\ E\{v_{Yki}\} = 0\,,$$

$$E\{v_{X_k t_i} v_{X_m t_j}\} = \delta_{ij} \sigma_{X_k X_m}\,,$$

$$E\{v_{Y_k t_i} v_{Y_m t_j}\} = \delta_{ij} \sigma_{Y_k Y_m}\,,$$

$$E\{v_{X_k t_i} v_{Y_m t_j}\} = \delta_{ij} \sigma_{X_k Y_m}\,. \tag{39}$$

In the first iteration we use a common unknown variance $\sigma_{X_k X_m} = \sigma_{Y_k Y_m} = \sigma_{X_k Y_m} = \delta_{km} \sigma^2$ and zero correlation between different coordinates, which allows separate linear regressions yielding residuals

$$\hat{v}_{X_k t_i} = X(P_k, t_i) - \hat{X}_{0k} - t_i \hat{U}_k$$

$$\hat{v}_{Y_k t_i} = Y(P_k, t_i) - \hat{Y}_{0k} - t_i \hat{V}_k\,. \tag{40}$$

For each point P_k the coordinate and velocity estimates are derived from the following algorithm

$$\bar{t} = \frac{1}{N} \sum_i t_i\,, \qquad m_t^2 = \frac{1}{N} \sum_i (t_i - \bar{t})^2$$

$$\bar{X}_k = \frac{1}{N} \sum_i X_{ki}\,,\ m_{tX,k} = \frac{1}{N} \sum_i (t_i - \bar{t})(X_{ki} - \bar{X}_k)\,,$$

$$\bar{Y}_k = \frac{1}{N} \sum_i Y_{ki}\,, \qquad m_{tY,k} = \frac{1}{N} \sum_i (t_i - \bar{t})(Y_{ki} - \bar{Y}_k)\,,$$

$$\hat{U}_k = \frac{m_{tX,k}}{m_t^2}, \qquad \hat{V}_k = \frac{m_{tY,k}}{m_t^2},$$

$$\hat{X}_{0k} = \overline{X}_k - \hat{U}_k \overline{t}\ , \quad \hat{Y}_{0k} = \overline{Y}_k - \hat{V}_k \overline{t}\ . \tag{41}$$

The residuals are utilized for the derivation of unbiased estimates

$$\hat{\sigma}_{X_k X_m} = \frac{1}{N-2}\sum_i \hat{v}_{X_k t_i}\hat{v}_{X_m t_i}\ ,$$

$$\hat{\sigma}_{Y_k Y_m} = \frac{1}{N-2}\sum_i \hat{v}_{Y_k t_i}\hat{v}_{Y_m t_i}\ ,$$

$$\hat{\sigma}_{X_k Y_m} = \frac{1}{N-2}\sum_i \hat{v}_{X_k t_i}\hat{v}_{Y_m t_i}\ , \tag{42}$$

which constitute an estimate for the common covariance matrix for each epoch to be used in the second iteration:

$$\hat{\boldsymbol{\Sigma}} = \begin{bmatrix} \hat{\sigma}^2_{X_1} & \cdots & \hat{\sigma}_{X_1 X_M} & \hat{\sigma}_{X_1 Y_1} & \cdots & \hat{\sigma}_{X_1 Y_M} \\ \vdots & \ddots & \vdots & \vdots & \ddots & \vdots \\ \hat{\sigma}_{X_M X_1} & \cdots & \hat{\sigma}^2_{X_M} & \hat{\sigma}_{X_M Y_1} & \cdots & \hat{\sigma}_{X_M Y_M} \\ \hat{\sigma}_{Y_1 X_1} & \cdots & \hat{\sigma}_{Y_1 X_M} & \hat{\sigma}^2_{Y_1} & \cdots & \hat{\sigma}_{Y_1 Y_M} \\ \vdots & \ddots & \vdots & \vdots & \ddots & \vdots \\ \hat{\sigma}_{Y_M X_1} & \cdots & \hat{\sigma}_{Y_M X_M} & \hat{\sigma}_{Y_1 Y_M} & \cdots & \hat{\sigma}^2_{Y_M} \end{bmatrix} \tag{43}$$

In the second iteration the linear regressions are performed simultaneously ordering the data as follows

$$\mathbf{b} = [\mathbf{b}^T_{X_1} \cdots \mathbf{b}^T_{X_M} \mathbf{b}^T_{Y_1} \cdots \mathbf{b}^T_{Y_M}]^T \tag{44}$$

with

$$\mathbf{b}_{X_k} = \begin{bmatrix} X(P_k, t_1) \\ \vdots \\ X(P_k, t_N) \end{bmatrix}, \quad \mathbf{b}_{Y_k} = \begin{bmatrix} Y(P_k, t_1) \\ \vdots \\ Y(P_k, t_N) \end{bmatrix}. \tag{45}$$

In the collective linear model $\mathbf{b} = \mathbf{A}\mathbf{x} + \mathbf{v}$, the residuals have covariance matrix of the form $\mathbf{C} = \boldsymbol{\Sigma} \otimes \mathbf{I}_N$. We utilize the estimate $\hat{\boldsymbol{\Sigma}}$ and set

$$\mathbf{C} = E\{\mathbf{v}\mathbf{v}^T\} = \kappa^2(\hat{\boldsymbol{\Sigma}} \otimes \mathbf{I}_N) \tag{46}$$

including an accommodating variance factor κ^2 and the adjustment is performed using a weight matrix

$$\mathbf{P} = (\hat{\boldsymbol{\Sigma}} \otimes \mathbf{I}_N)^{-1} = \hat{\boldsymbol{\Sigma}}^{-1} \otimes \mathbf{I}_N = \mathbf{W} \otimes \mathbf{I}_N \tag{47}$$

where

$$\mathbf{W} = \begin{bmatrix} \mathbf{W}_X & \mathbf{W}_{XY} \\ \mathbf{W}^T_{XY} & \mathbf{W}_Y \end{bmatrix} = \hat{\boldsymbol{\Sigma}}^{-1}. \tag{48}$$

It can be shown that the solution breaks down into individual linear regressions leading to the same estimates as in the first step. The only difference is in the covariance propagation step which is performed by first computing the estimate of the variance factor

$$\begin{aligned} \hat{\mathbf{v}}^T\mathbf{P}\hat{\mathbf{v}} = &\sum_{k,m,i} (\mathbf{W}_X)_{km}\hat{v}_{X_k t_i}\hat{v}_{X_m t_i} + \\ &+ \sum_{k,m,i} (\mathbf{W}_{XY})_{km}\hat{v}_{X_k t_i}\hat{v}_{Y_m t_i} + \\ &+ \sum_{k,m,i} (\mathbf{W}^T_{XY})_{km}\hat{v}_{Y_m t_i}\hat{v}_{X_k t_i} + \\ &+ \sum_{k,m,i} (\mathbf{W}_Y)_{km}\hat{v}_{Y_k t_i}\hat{v}_{Y_m t_i}\ , \end{aligned} \tag{49}$$

$$\hat{\kappa}^2 = \frac{\hat{\mathbf{v}}^T\mathbf{P}\hat{\mathbf{v}}}{2(N-2)M} \tag{50}$$

and then the variances and covariances from

$$\hat{\sigma}_{\hat{X}_{0k}\hat{X}_{0m}} = \hat{\kappa}^2\,\hat{\sigma}_{X_k X_m}\frac{m_t^2 + \overline{t}^2}{N m_t^2},$$

$$\hat{\sigma}_{\hat{X}_{0k}\hat{Y}_{0m}} = \hat{\kappa}^2\,\hat{\sigma}_{X_k Y_m}\frac{m_t^2 + \overline{t}^2}{N m_t^2},$$

$$\hat{\sigma}_{\hat{Y}_{0k}\hat{Y}_{0m}} = \hat{\kappa}^2\,\hat{\sigma}_{Y_k Y_m}\frac{m_t^2 + \overline{t}^2}{N m_t^2}, \tag{51}$$

$$\hat{\sigma}_{\hat{U}_k\hat{U}_m} = \hat{\kappa}^2\,\hat{\sigma}_{X_k X_m}\frac{1}{N m_t^2},$$

$$\hat{\sigma}_{\hat{V}_k\hat{V}_m} = \hat{\kappa}^2\,\hat{\sigma}_{Y_k Y_m}\frac{1}{N m_t^2},$$

$$\hat{\sigma}_{\hat{U}_k\hat{V}_m} = \hat{\kappa}^2\,\hat{\sigma}_{X_kY_m}\,\frac{1}{Nm_t^2}\,, \tag{52}$$

$$\hat{\sigma}_{\hat{X}_{0k}\hat{U}_m} = -\hat{\kappa}^2\,\hat{\sigma}_{X_kX_m}\,\frac{\overline{t}}{Nm_t^2}\,,$$

$$\hat{\sigma}_{\hat{X}_{0k}\hat{V}_m} = -\hat{\kappa}^2\,\hat{\sigma}_{X_kY_m}\,\frac{\overline{t}}{Nm_t^2}\,,$$

$$\hat{\sigma}_{\hat{Y}_{0k}\hat{U}_m} = -\hat{\kappa}^2\,\hat{\sigma}_{Y_kX_m}\,\frac{\overline{t}}{Nm_t^2}\,,$$

$$\hat{\sigma}_{\hat{Y}_{0k}\hat{V}_m} = -\hat{\kappa}^2\,\hat{\sigma}_{Y_kY_m}\,\frac{\overline{t}}{Nm_t^2}\,. \tag{53}$$

Note that the above formulas are greatly simplified when the reference epoch t_0 is chosen so that $\overline{t} = 0$. The obtained velocity component estimates $\hat{U}_k$, $\hat{V}_k$ at each network point P_k must be interpolated to obtain a continuous velocity field $\mathbf{v} = \mathbf{v}(\mathbf{x}_0)$, where $\mathbf{x}_0 = [X_0\ Y_0]^T$ and $\mathbf{v} = [U\ V]^T$ from which the velocity gradient

$$\mathbf{L}_0 = \frac{\partial \mathbf{v}}{\partial \mathbf{x}_0} \tag{54}$$

referring to the reference epoch t_0 can be calculated. The displacements $\mathbf{u}$ between epoch t_0 and any other epoch t are given by $\mathbf{u}(t_0,t) = (t-t_0)\mathbf{v}$ and the displacement gradient is simply $\mathbf{J}(t_0,t) = (t-t_0)\mathbf{L}_0$. Thus the deformation gradient becomes

$$\mathbf{F}(t_0,t) = \mathbf{I} + \mathbf{J}(t_0,t) = \mathbf{I} + (t-t_0)\mathbf{L}_0\,. \tag{55}$$

Once the deformation gradient is calculated the deformation analysis can be performed as previously described. When the finite element method is used, instead of the displacements $\mathbf{u}$ one may interpolate the velocities $\mathbf{v}$, in which case the resulting matrix is not $\mathbf{J}$ but $\mathbf{L}_0$. For this reason we have used the same symbols (U, V) for both displacement and velocity components, while the equations (35) for the computation of the elements of $\mathbf{J}$ can be used for the computation of the corresponding elements of $\mathbf{L}_0$.

It is also possible to perform the deformation analysis for any pair of epochs t_1, t_2 considering that

$$\mathbf{F}(t_1,t_2) = \frac{\partial \mathbf{x}_2}{\partial \mathbf{x}_1} = \frac{\partial \mathbf{x}_2}{\partial \mathbf{x}_0}\frac{\partial \mathbf{x}_0}{\partial \mathbf{x}_1} = \frac{\partial \mathbf{x}_2}{\partial \mathbf{x}_0}\left(\frac{\partial \mathbf{x}_1}{\partial \mathbf{x}_0}\right)^{-1} =$$

$$= \mathbf{F}(t_0,t_2)\mathbf{F}(t_0,t_1)^{-1} =$$

$$= [\mathbf{I} + (t_2-t_0)\mathbf{L}_0][\mathbf{I} + (t_1-t_0)\mathbf{L}_0]^{-1}\,. \tag{56}$$

Taking into account that for a "small" matrix $\mathbf{\Delta}$ $(\mathbf{I}+\mathbf{\Delta})^{-1} \cong \mathbf{I} - \mathbf{\Delta}$, we may use the approximation

$$\mathbf{F}(t_1,t_2) \approx \mathbf{I} + (t_2-t_1)\mathbf{L}_0\,. \tag{57}$$

The velocity gradient at any epoch t is given by

$$\mathbf{L} = \mathbf{L}(t) = \frac{\partial \mathbf{v}}{\partial \mathbf{x}} = \frac{\partial \mathbf{v}}{\partial \mathbf{x}_0}\frac{\partial \mathbf{x}_0}{\partial \mathbf{x}} = \mathbf{L}_0\mathbf{F}(t_0,t)^{-1} =$$

$$= \mathbf{L}_0[\mathbf{I} + (t-t_0)\mathbf{L}_0]^{-1} \approx \mathbf{L}_0 \tag{58}$$

and it can be used to derive the corresponding symmetric "stretch" or "rate-of-strain" matrix

$$\mathbf{D} = \frac{1}{2}(\mathbf{L} + \mathbf{L}^T) \tag{59}$$

and the antisymmetric "spin" matrix

$$\mathbf{W} = \tfrac{1}{2}(\mathbf{L} - \mathbf{L}^T) = \begin{bmatrix} 0 & w \\ -w & 0 \end{bmatrix}, \quad w = \frac{L_{12} - L_{21}}{2}\,. \tag{60}$$

6 A Numerical Example

For a numerical illustration of the proposed methodology, we consider a network of permanent GPS stations (fig. 1) covering a region separated in two parts by a fault. Coordinate time series have been simulated for a time span of two years, applying linear velocities of the order of some cm/year to the station coordinates. Moreover, two rigid transformations, linear with respect to time, with the same order of magnitude of the velocities, have been added to the data: a first one on the right (R) network alone, to simulate a tectonic effect of that region with respect to the other; the second one on both networks, to simulate a reference frame effect. At the end, a realistic noise (of the order of some mm) has been added to the coordinates.

We shall derive the motion (displacements in X, Y and rotation) for the whole region, and each one of the separate parts (subregions) with respect to the

global reference system (WGS84 or ITRF) used in GPS data analysis, as well as the relative motion of one subregion with respect to the other. Within each subregion a deformation analysis is performed using the finite element interpolation method, which leads to estimates of deformation parameters and their standard deviations and correlation. These statistics are based on the previously described variance-covariance analysis and are independent from the unrealistic formal statistics derived within the adjustment of the GPS observations.

The motion of a network covering a deforming region is derived by defining its corresponding "Tisserand" reference system, which best represents the network as a whole, by preserving the "center of mass" of the network points (considered as material points with unit mass) and by the vanishing of their relative angular momentum (Dermanis & Kotsakis, 2005). In the planar case the original coordinates X, Y are transformed into new coordinates $\tilde{X}$, $\tilde{Y}$ by a (counter-clockwise) rotation θ and displacements d_X, d_Y (all functions of time) by requiring that

$$\sum_k \tilde{X}_k = \sum_k \tilde{Y}_k = 0 \tag{61}$$

$$\tilde{h} = \sum_k (\tilde{X}_k \tilde{V}_k - \tilde{Y}_k \tilde{U}_k) = 0 \tag{62}$$

for the conservation of the center of mass and the vanishing of the relative angular momentum $\tilde{h}$, respectively. For linearly varying coordinates the solution is given by

$$\theta(t) = \theta_0 + \frac{h_0}{2\sqrt{S_v^2 S_0^2 - S_{0v}^2}} \arctan \frac{S_v^2 t + S_{0v}}{\sqrt{S_v^2 S_0^2 - S_{0v}^2}} \tag{63}$$

$$\begin{bmatrix} d_X(t) \\ d_Y(t) \end{bmatrix} = -\begin{bmatrix} \cos\theta(t) & \sin\theta(t) \\ -\sin\theta(t) & \cos\theta(t) \end{bmatrix} \begin{bmatrix} m_{0X} + t\, m_U \\ m_{0Y} + t\, m_V \end{bmatrix} \tag{64}$$

where

$$m_{0X} = \frac{1}{N}\sum_k X_{0k}\,, \qquad m_{0Y} = \frac{1}{N}\sum_k Y_{0k}\,,$$
$$m_U = \frac{1}{N}\sum_k U_k\,, \qquad m_V = \frac{1}{N}\sum_k V_k\,; \tag{65}$$

$$\Delta X_{0k} = X_{0k} - m_{0X}\,, \qquad \Delta Y_{0k} = Y_{0k} - m_{0Y}\,,$$
$$\Delta U_k = U_k - m_U\,, \qquad \Delta V_k = V_k - m_V\,, \tag{66}$$

$$S_0^2 = \frac{1}{N}\sum_k (\Delta X_{0k}^2 + \Delta Y_{0k}^2)\,, \tag{67}$$

$$S_{0v} = \frac{1}{N}\sum_k (\Delta X_{0k}\Delta U_k + \Delta Y_{0k}\Delta V_k)\,, \tag{68}$$

$$S_v^2 = \frac{1}{N}\sum_k (\Delta U_k^2 + \Delta V_k^2) \tag{69}$$

$$h_0 = \frac{1}{N}\sum_k (\Delta X_k \Delta V_k - \Delta Y_k \Delta U_k)\,. \tag{70}$$

Using the computed parameters $\theta(t)$, $d_X(t)$, $d_Y(t)$, the station coordinates within each subregion can be transformed from the original global frame to the corresponding Tisserand frame, so that any common displacement and rotational trend is removed before performing the deformation analysis.

A noticeable property of such a reference system transformation (where a generally different time dependent transformation is performed on the coordinates of each epoch), is that the property of linear coordinate variation is not preserved from a strictly theoretical point of view. In fact this linear model of reference epoch coordinates and constant velocities, so widely used (e.g. in the formulation of the ITRF) has no solid theoretical foundation. Despite common belief, there exists no such thing as an intrinsic (coordinate-free) linear in time deformation of the network! From a practical point of view though we may limit ourselves to small displacements and rotations, in which case we can use instead of (63) the approximation $\theta(t) \approx \theta' t$ (with $\theta_0 = 0$), where

$$\theta' \equiv \frac{d\theta}{dt} \approx \frac{h_0}{S_0^2}\,. \tag{71}$$

with the same degree of approximation the displacements are $d_X(t) = t\, d'_X$, $d_Y(t) = t\, d'_Y$, with constant displacement velocities

$$d'_X \equiv \frac{d(d_X)}{dt} \approx -m_U - \theta' m_{0Y}$$

$$d'_Y \equiv \frac{d(d_Y)}{dt} \approx -m_Y + \theta' m_{0X} \qquad (72)$$

The values of the time derivatives θ', d'_X, d'_Y characterize the motion of the subregion as a whole, as represented by its own Tisserand frame. The computed values for the two regions in the left (L) of the fault and in the right (R) of the fault as well as for the whole network (L+R) are presented in the following table

	d'_X (m/y)	d'_Y (m/y)	θ' (″/y)
L+R	0.0369	0.0067	–0.64
L	0.0349	0.0102	–0.74
R	0.0285	0.0353	–0.48
R–L	–0.0064	0.0251	0. 26

Table 1: Displacement components and angular velocity of network regions and subregions

Of particular importance are the first row (L+R) which represents the motion of the whole region with respect to the global network, as well as the last one (R–L), which represents the relative motion of the right subregion with respect to the left one. The network of the whole region moves in a north-east direction with a velocity of 3.75 cm/year (eastern component 3.7 cm/year - northern component 0.7 cm/year) and rotates around its own mass center clock-wise with angular velocity of 0.64″/year.

Considering Tisserand system of the left region as constant, the network of the right region moves in a north-west direction with a velocity of 2.6 cm/year (western component 0.6 cm/year - northern component 2.5 cm/year) and rotates around its own mass center counter-clock-wise with angular velocity of 0.26″/year.

After the removal of the trend due to the definition of the reference frame the velocities of all stations, (each one referring to the Tisserand frame of its own subregion) are depicted in fig. 1.

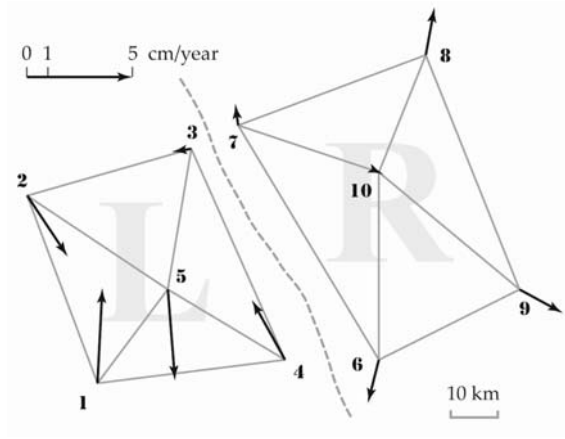

Fig. 1: The network of permanent GPS stations and the remaining velocities after the removal of trend due to the reference system definition

pt	X_0 (m)	Y_0 (m)	U (mm/y)	V (mm/y)
1	–11999.9176	–23000.0431	2.3	45.1
2	–27000.0610	16999.9033	19.2	–28.8
3	7999.9034	27000.0286	3.4	–43.2
4	28000.0646	–17999.8997	–15.7	28.3
5	3000.0107	–2999.9891	–9.2	–1.4
6	–1999.9211	–34000.0047	–5.2	–20.5
7	–32000.0370	15999.9259	–1.4	10.2
8	7999.9281	31000.0184	4.1	22.5
9	28000.0442	–18999.9351	20.5	–11.2
10	–2000.0141	5999.9955	2.0	–0.9

Table 2: Estimated reference-epoch coordinates and velocity components

point	σ_{X_0} (mm)	σ_{Y_0} (mm)	σ_U (mm/y)	σ_V (mm/y)
1	0.12	0.16	0.20	0.28
2	0.11	0.12	0.19	0.20
3	0.17	0.16	0.29	0.27
4	0.13	0.17	0.23	0.29
5	0.14	0.11	0.25	0.20
6	0.17	0.11	0.30	0.20
7	0.12	0.18	0.20	0.31
8	0.17	0.13	0.29	0.23
9	0.18	0.12	0.31	0.20
10	0.16	0.13	0.28	0.22

Table 3: Standard deviations of the estimated reference epoch coordinates and velocity components

The results of the finite element deformation analysis are listed in tables 4 and 5 and are depicted in figures 2 and 3. Figure 2 depicts the values of $1+k(\lambda_i-1)$, as the semi-axes of an ellipse compared to a unit circle. The semi-axes are oriented according to their computed directions (angle θ_P and θ_P+90°). The exaggeration factor is $k=0.25\times10^6$. Figure 3 depicts the direction of maximal shear by an oriented (angle ϕ) line segment having $\gamma\times10^{-6}$ as its length. Dilatation Δ is depicted by a circle with radius $R=\sqrt{1+k\Delta}$ compared to a unit circle, with an exaggeration factor of $k=0.25\times10^6$.

The standard deviations and correlations of the deformation parameters are given in tables 6, 7 and 8. In tables 7 and 8, the upper triangular part contains the correlations between λ_1, λ_2 and θ_P, while the lower triangular part contains the correlation between γ, Δ and ϕ.

triangle	$(\lambda_1-1)\times10^6$	$(\lambda_2-1)\times10^6$	θ_P (°)
1-5-2	-0.862	-2.031	8.313
2-5-3	-0.526	-1.465	-16.303
3-5-4	0.083	-1.536	-13.623
4-5-1	-0.395	-2.240	6.335
6-10-7	0.841	0.489	2.178
7-10-8	1.010	0.659	66.990
8-10-9	0.838	0.482	-72.339
9-10-6	0.813	0.444	-20.763

Table 4: Principal extensions and their direction

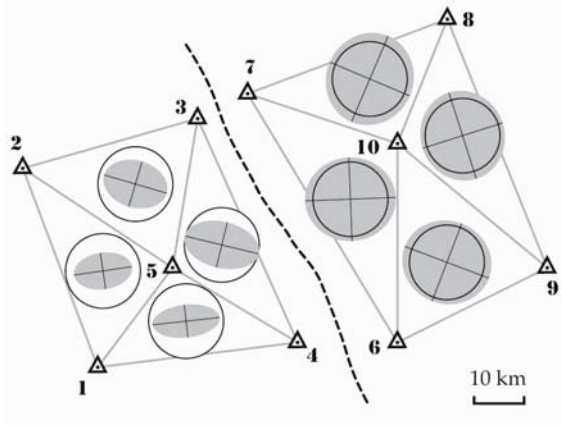

Fig. 2: Principal extensions and their directions.

triangle	$\gamma\times10^6$	$\Delta\times10^6$	ϕ (°)
1-5-2	1.169	-2.893	53.313
2-5-3	0.939	-1.991	61.303
3-5-4	1.619	-1.454	58.623
4-5-1	1.846	-2.635	51.335
6-10-7	0.351	1.330	47.178
7-10-8	0.351	1.669	111.990
8-10-9	0.355	1.320	117.339
9-10-6	0.370	1.257	65.763

Table 5: Dilatation, maximum shear and its direction

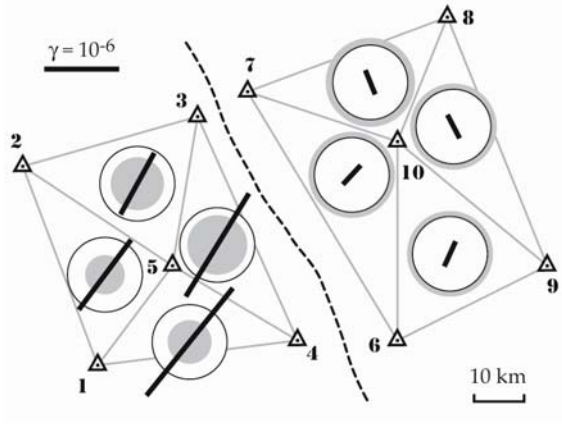

Fig. 3: Dilatation, maximum shear and its direction

triang.	σ_{λ_1} ($\times10^6$)	σ_{λ_2} ($\times10^6$)	σ_{θ_P} (deg)	σ_γ ($\times10^6$)	σ_Δ ($\times10^6$)	σ_ϕ (deg)
1-5-2	0.012	0.010	0.360	0.015	0.017	0.360
2-5-3	0.009	0.008	0.412	0.012	0.013	0.412
3-5-4	0.016	0.006	0.249	0.018	0.017	0.249
4-5-1	0.006	0.013	0.265	0.015	0.015	0.265
6-10-7	0.012	0.007	1.278	0.014	0.014	1.278
7-10-8	0.013	0.007	1.150	0.016	0.013	1.150
8-10-9	0.009	0.013	1.203	0.016	0.015	1.203
9-10-6	0.012	0.007	0.964	0.014	0.014	0.964

Table 6: Standard deviations of the deformation parameters

		1 - 5 - 2			2 - 5 - 3			3 - 5 - 4			4 - 5 - 1				
		λ_1	λ_2	θ_P	λ_1	λ_2	θ_P	λ_1	λ_2	θ_P	λ_1	λ_2	θ		
1	γ		0.14	0.59	0.36	0.22	-0.64	-0.72	0.07	0.03	-0.28	0.21	0.78	λ_1	1
5	Δ	0.16		0.63	-0.12	-0.15	-0.12	-0.13	-0.06	-0.23	0.25	0.85	0.45	λ_2	5
2	ϕ	0.03	0.80		0.08	-0.25	-0.31	-0.54	-0.06	-0.29	0.04	0.75	0.70	θ_P	2
2	γ	0.09	0.09	0.24		0.08	0.19	0.15	0.24	0.30	-0.02	0.04	0.02	λ_1	2
5	Δ	0.46	0.17	-0.10	0.08		0.28	-0.02	0.75	0.83	-0.14	-0.41	0.30	λ_2	5
3	ϕ	-0.44	-0.53	-0.31	-0.05	0.31		0.69	0.54	0.54	0.26	-0.18	-0.43	θ_P	3
3	γ	-0.49	-0.55	-0.47	0.24	-0.15	0.44		-0.04	0.29	0.68	-0.34	-0.54	λ_1	3
5	Δ	-0.43	-0.55	-0.53	-0.01	0.33	0.85	0.73		0.57	-0.21	-0.04	-0.00	λ_2	5
4	ϕ	0.18	-0.12	-0.29	-0.36	0.75	0.54	0.06	0.49		-0.03	-0.52	0.22	θ_P	4
4	γ	0.22	-0.63	-0.67	-0.26	0.18	0.28	0.56	0.54	0.46		0.01	-0.03	λ_1	4
5	Δ	-0.55	0.59	0.70	0.33	-0.26	-0.06	0.02	-0.07	-0.48	-0.67		0.26	λ_2	5
1	ϕ	0.32	0.82	0.70	-0.20	0.21	-0.43	-0.49	-0.51	0.22	-0.25	0.22		θ_P	1
		γ	Δ	ϕ	γ	Δ	ϕ	γ	Δ	ϕ	γ	Δ	ϕ		
		1 - 5 - 2			2 - 5 - 3			3 - 5 - 4			4 - 5 - 1				

Table 7: Correlations between deformation parameters for the left sub-region

		6 - 10 - 7			7 - 10 - 8			8 - 10 - 9			9 - 10 - 1				
		λ_1	λ_2	θ_P	λ_1	λ_2	θ_P	λ_1	λ_2	θ_P	λ_1	λ_2	θ_P		
6	γ		0.01	0.60	0.39	0.28	0.77	-0.14	-0.71	0.60	0.13	-0.43	0.53	λ_1	6
10	Δ	0.49		0.52	-0.52	0.02	0.19	-0.49	0.23	0.16	0.39	0.72	0.43	λ_2	10
7	ϕ	0.25	0.78		-0.35	0.39	0.45	-0.39	-0.22	0.44	0.35	0.13	0.44	θ_P	7
7	γ	0.39	-0.05	-0.46		-0.20	0.10	0.57	-0.61	0.14	-0.03	-0.73	0.24	λ_1	7
10	Δ	0.70	0.20	-0.13	0.55		-0.20	0.36	0.10	-0.28	-0.05	0.01	-0.02	λ_2	10
8	ϕ	0.57	0.76	0.45	0.17	-0.01		-0.68	-0.55	0.76	0.07	-0.13	0.44	θ_P	8
8	γ	0.65	0.18	-0.05	0.60	0.85	0.04		-0.05	-0.47	-0.12	-0.40	-0.15	λ_1	8
10	Δ	-0.53	-0.63	-0.42	-0.26	-0.00	-0.86	-0.31		-0.57	0.29	0.66	-0.66	λ_2	10
9	ϕ	0.44	0.60	0.44	0.24	-0.02	0.76	0.18	-0.76		-0.20	0.04	0.23	θ_P	9
9	γ	0.29	0.27	0.25	0.29	0.30	0.13	0.11	-0.00	-0.20		0.03	0.21	λ_1	9
10	Δ	-0.44	0.26	0.37	-0.30	-0.39	-0.01	-0.63	0.29	-0.15	0.51		-0.27	λ_2	10
1	ϕ	0.24	0.67	0.44	0.21	0.22	0.44	0.43	-0.63	0.23	0.32	0.05		θ_P	1
		γ	Δ	ϕ	γ	Δ	ϕ	γ	Δ	ϕ	γ	Δ	ϕ		
		6 - 10 - 7			7 - 10 - 8			8 - 10 - 9			9 - 10 - 1				

Table 8: Correlations between deformation parameters for the right sub-region

Conclusions

Despite some simplified assumptions on the variance-covariance structure of the data, a consistent and rigorous approach has been formalized to infer network deformations from continuous time series of coordinates. The proposed approach allows also the evaluation of both the accuracies and the correlations of the estimated parameters.

The numerical example shows that by the proposed empirical approach, a realistic estimate of the network covariance matrix is possible. The Tisserand approach, applied to the linear trends estimated from the original coordinate series, provides the estimate of the global motion of a region (reference frame effects) as well as the relative motion of two regions (relative tectonic effects).

The estimated standard deviations and correlations of the deformation parameters provide useful information in the deformation analysis; for exam-

ple, in the case study, all the direction parameters of network *L* are characterized by smaller standard deviations than the corresponding of network *R*: this is due to the nature of the deformations in the *R* region, that are practically homogeneous.

With regard to the principal extension parameters, the smaller correlations within each triangle are between λ_1 and λ_2; with regard to dilatation, maximum shear and the related angle, the same holds for γ and Δ. Generally, adjacent triangles show the highest correlations.

All the algorithms have been implemented in a software package, written in standard C language. After some minor refinements it will become available to the scientific community.

Acknowledgements

L. Biagi's work has been supported by the "Satellite Positioning Services for the e-government" Italian PRIN 2004 project.

References

Dermanis, A. & E. Livieratos (1983): Applications of Deformation Analysis in Geodesy and Geodynamics. *Reviews of Geophysics and Space Physics*, vol. 51, no. 1, 41-50.

Dermanis, A. and D. Rossikopoulos (1988): Modeling Alternatives in Four-Dimensional Geodesy. Proceedings of the International Symposium "*Instrumentation, Theory and Analysis for Integrated Geodesy*", Sopron, Hungary, May 16-20, 1988, Vol. 2, 115-145.

Dermanis, A. (1994): A method for the determination of crustal deformation parameters and their accuracy from distances. *Journal of the Geodetic Society of Japan*, vol. 40, no. 1, 17-32.

Rossikopoulos, D. (2001): Modeling Alternatives in Deformation Measurements. In: A. Carosio & H. Kutterer (eds.) "*First International Symposium on Robust Statistics and Fuzzy Techniques in Geodesy and GIS*", ETH Zurich, Inst. of Geodesy and Photogrametry, No. 295.

Dermanis, A and C. Kotsakis (2005): Estimating crustal deformation parameters from geodetic data: Review of existing methodologies, open problems and new challenges. In these proceedings.